Canadian Metallurgical Quarterly, Vol 48, No 2 pp 177-186, 2009
© Canadian Institute of Mining, Metallurgy and Petroleum
Published by Canadian Institute of Mining, Metallurgy and Petroleum
Printed in Canada. All rights reserved

EFFECT OF MAGNESIA ADDITION ON PHYSICAL PROPERTIES AND SLAG ATTACK RESISTANCE OF ULTRA-LOW CEMENT CASTABLES (ULC)

Y. KUTMEN KALPAKLI[1] and **S. YILMAZ**[2]

[1]Yildiz Technical University, Faculty of Chemistry and Metallurgy,
Department of Chemical Engineering, Istanbul, Turkey
yaseminkalpakli@gmail.com
[2]Istanbul University, Faculty of Engineering,
Department of Metallurgical and Materials Engineering, Istanbul, Turkey

(Received in revised form March, 2009)

Abstract — In this study, tabular alumina and seawater magnesia were used to synthesize *in situ* Al_2O_3-MgO spinel castables. Secar® 71 cement was used as a binder. In order to produce *in situ* formation of Al_2O_3-MgO spinel castables, the effect of MgO content on refractory properties was investigated by adding to the mixture at the proportions of 3, 4, 5, 6, 7 wt%. Using 5 wt% content of MgO decreased the bulk density of castables to 3.03 g/cm^3 and increased the porosity to about 17.43%. *In situ* spinel formation in samples led to the expansion in its lattice as well as an increase in the porosity. On the other hand, 5 wt% MgO had a positive effect on Cold Crushing Strength (CCS) of the castable. SEM investigations of fired samples were carried out to compare the effect of MgO addition and *in situ* phase formation on the physico-mechanical properties of castables. The effect of MgO content on the mechanism of slag penetration of ultra-low cement castables **(**ULC) for steel ladles was examined and the penetration layer was chemically analyzed.

Résumé — Dans cette étude, on a utilisé de l'alumine tabulaire et de la magnésie d'eau de mer pour synthétiser *in situ* des bétons réfractaires de spinelle Al_2O_3-MgO. On a utilisé le ciment Secar® 71 comme liant. Afin d'obtenir la formation *in situ* de bétons réfractaires de spinelle Al_2O_3-MgO, on a étudié l'effet de la teneur en MgO sur les propriétés réfractaires en l'ajoutant au mélange à des proportions de 3, 4, 5, 6, et 7% en poids. Une teneur de 5% en poids de MgO diminuait la densité apparente des réfractaires à 3.03 g/cm^3 et augmentait la porosité à environ 17.43%. La formation de spinelle *in situ* dans les échantillons menait à l'expansion de son réseau ainsi qu'à une augmentation de la porosité. D'un autre côté, 5% en poids de MgO avait un effet positif sur la résistance à la compression à froid (CCS) du réfractaire. On a effectué des études de SEM d'échantillons cuits pour comparer l'effet d'addition de MgO et la formation de phase *in situ* sur les propriétés physico-mécaniques des réfractaires. On a examiné l'effet de la teneur en MgO sur le mécanisme de pénétration des scories des réfractaires à ultra-basse teneur en ciment (ULC) pour les poches de coulée d'acier et l'on a analysé chimiquement la couche de pénétration.

INTRODUCTION

The need for the production of high quality steel particularly necessitates the selection of high quality castables which can be used in the presence of molten slag and metals. In view of the increasing demand for these materials, there is heightened interest in their physical, chemical and thermomechanical properties of these materials [1,2]. Today, refractory cement bound spinel-alumina castables are popular materials because they have superior slag corrosion and metal erosion strength [3,4]. On the other hand, magnesia-chrome bricks used in the cement ovens, create harmful solid wastes for the environment and cause magnesia-spinel materials to be preferred due to the carcinogen effect of Cr^{+6} inside the structure of magnesia-chrome bricks [5].

Magnesia is used as an additive material (dead burned or seawater magnesia) for production of *in situ* spinel high alumina refractory castables by reactive sintering. This type of spinel has an even greater resistance to corrosion and slag penetration in comparison with high alumina concretes with added synthetic spinel [6,7]. However, the use of magnesia presents certain disadvantages due to hydration and other associated rheological problems [8-10].

Alumina rich refractory concretes are currently used in the steel industry as an added synthetic spinel or *in situ* spinel formation. Using compositions in the high alumina zone of Al_2O_3- MgO-CaO ternary phase equilibrium diagram provides two significant advantages to the users. Firstly, it has high invariant points with temperatures generally above 1700 °C and makes it possible to produce highly refractory materials. Moreover, concrete designed in this composition range will show low solubility against molten product, due to the broad primary crystallization field of $MgAl_2O_4$ spinel. Additionally, spinel is a crystalline phase that absorbs a large amount of metal cations (Fe^{+2}, Fe^{+3}, Mn^{+2}) into its structure, forming a wide range of solid solutions [11-17].

As the content of high alumina cement used as a hydraulic binder increases in the composition of castables, the water content needed for a good setting rises as well. Thus, the resistance against the slag penetration of the product which has high porosity content is low [18]. Today, low and ultra-low cement castables are widely used because of their excellent refractory properties and simple applicability [19]. In castables where calcium aluminate cement is used as a binder, the microstructure exchange occurring during sintering is explained quite clearly with the studies [20]. As a result of the hydration reaction, calcium aluminate hydrates which have different morphologies depending on water/cement ratio, mixture conditions (particularly heat and relative moisture) and impurity are formed. All hydrate components are exposed to dehydration at 550 °C [21] and active lime and alumina, which are dry products, produce Calcium Aluminate by being shaped. The thin fraction of matrix phase contains hydration products. These hydration products both react among themselves and the hydration or reaction products of those can react with thicker agrera phase when being raised to higher temperatures. $C_{12}A_7$, CA and CA_2 in turn are formed through the heat rise to 1300 °C in the castables with conventional cement binders. Hexagonal CA_6 whose melting point is the highest calcium-aluminate phase takes shape through CA_2 reaction with alumina [22]. Hydration reactions form quite rapidly. This situation is a significant advantage in the industrial applications. The existence of $C_{12}A_7$ affects the rapid solidification features of refractory significantly. In the castable refractory which cement is used as hydraulic binder, 'CaO' in cement composition affects the features of refractory at high temperature in a negative way. Therefore, 'Low Cement' of which CaO content is between 1<%CaO<2.5 and 'Ultra-Low Cement' with CaO content of 0.2<%CaO<1 are being used in castables [18].

In this work, different proportions of seawater magnesia were added to the mixture as a source of magnesia and *in situ* formation of Mg Al_2O_4 spinel was investigated at 1500 °C and 1600 °C. Optimum sintering temperature and proportion of seawater magnesia were determined by using physical and XRD analysis of castables. The effect of slag penetration on the product was investigated.

EXPERIMENTAL PROCEDURE

Properties of Raw Materials

In this work, alumina from Almatis Industrial Chemicals, Germany having various particle sizes and seawater magnesia from China were added to the blend as starting materials. Secar®71 calcium aluminate cement was used as a binder. The chemical composition and physical properties of tabular alumina, Secar®71 calcium aluminate cement, silica fume and seawater magnesia are given Tables I and II.

Table I – The chemical composition and physical properties of tabular alumina and Secar-71 calcium aluminates cement

Raw materials	Chemical composition	(%)
Secar®71 calcium aluminates cement	CaO	27
	Al_2O_3	72
	Na_2O	Max: 0.30
	SiO_2	Max: 0.30
	Fe_2O_3	Max: 0.20
	MgO	Max: 0.40
Tabular alumina	Al_2O_3	>99.4
	Na_2O	0.60
	SiO_2	≤0.12
	Fe_2O_3	≤0.30
	Physical properties	
	Bulk specific gravity (g/cm^3)	≥3.5
	Apparent porosity (%)	≤ 5
	Water adsorption (%)	≤1.5

Table II – Chemical composition of seawater magnesia and hydratable alumina

Raw Materials	Composition	(%)
Seawater magnesia	MgO	99.36
	Fe_2O_3	0.20
	SiO_2	0.14
Micro silica	SiO_2	97.00
	SiC	0.50
	MgO	0.30
	Al_2O_3	0.15
	CaO	0.20
	Na_2O	0.05
	K_2O	0.80
	Fe_2O_3	0.03

The particle size distributions of tabular alumina, reactive alumina, calcined alumina, silica fume and Secar®71 calcium aluminates cement which were added into the mixture as super fines are displayed in Figure 1. The particle size distributions of ADS1 and ADW1 were added into the mixture by using coordination of blend solidification point. These results are also given in Figure 1. The particle size distribution analyses of these materials were done using a Malvern™ Mastersizer 2000 instrument.

Preparation of Samples

The Andreassen equation [23,24] was used to determine the ratio of the range of the particle size of the raw material and particle size distribution parameter (q) was found to be 0.26 for vibratory castables in a previous study [25]. The mixtures were prepared by using the particle size distribution parameter q=0.26. Various proportions of seawater magnesia

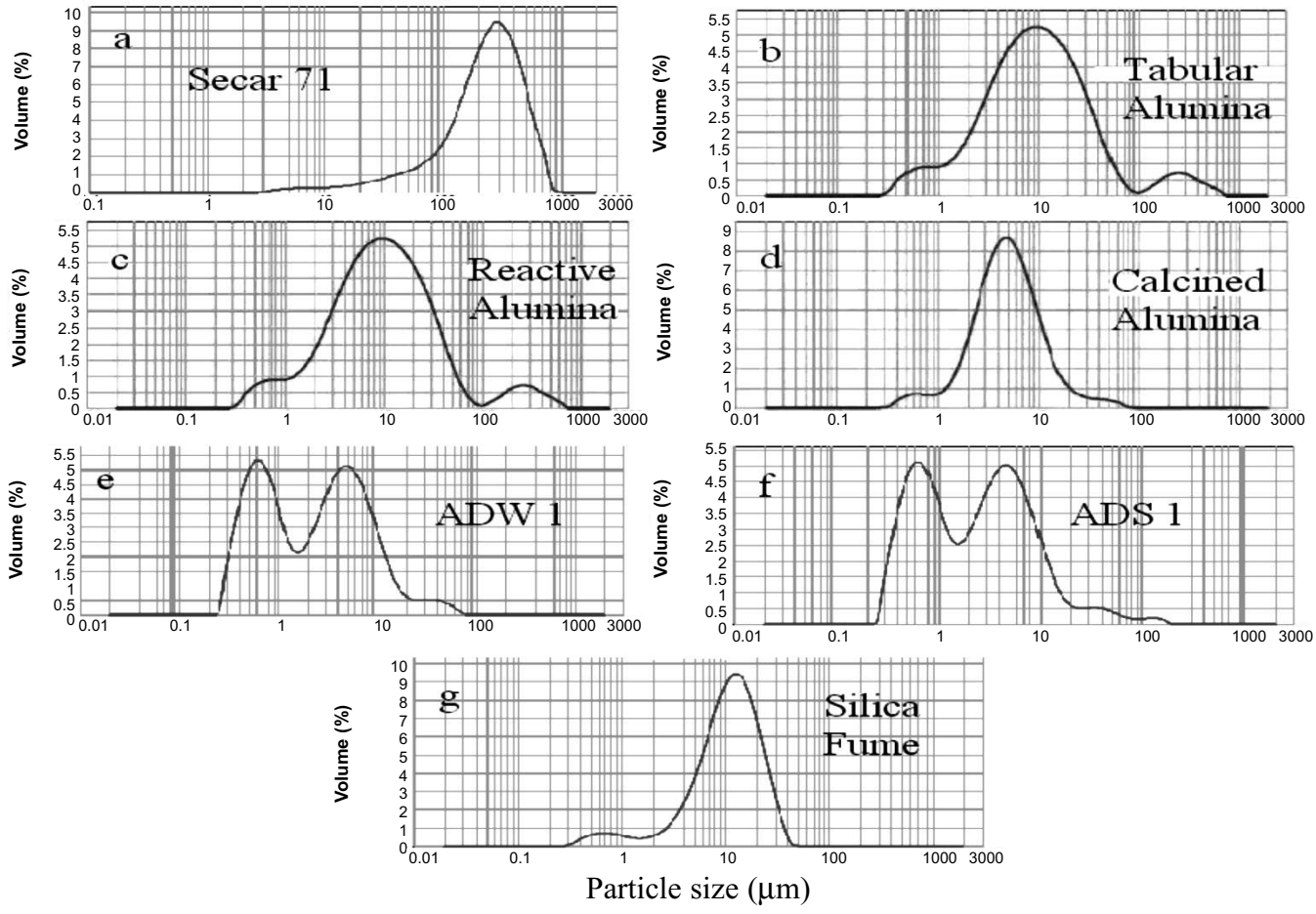


Fig. 1. Particle size distributions of a) Secar® 71, b) Tabular alumina (0-0.045 mm), c) Reactive alumina, d) Calcined alumina, e) ADW1, f) ADS1, g) Micro silica.

(3, 4, 5, 6 and 7 wt% of MgO given names as M3, M4, M5, M6, M7) were added to this mixtures for composed *in situ* $MgAl_2O_4$ spinel formation.

Particle size ranges and mass contents of these mixtures are listed in Table III. Firstly, each mixture was dry mixed in a Hobart™ A200 mixer for 2 minutes. Then water was added to the pre-mixed blend and wet mixing was carried out for about 5 minutes. The homogenized mixture was cast into moulds of 5×5×5 cm^3 onto a vibrating table with 50 Hz vibrating rate. The samples were kept for 24 hours at room temperature and then cured at a temperature of 110 °C for 24 hrs in a Binder type incubator. The refractory samples were sintered in two different groups at a temperature of 1500 and 1600 °C for five hours in a NaberTherm™ Germany-type controlled direct heater furnace at heating speed of 5 °C/min. After firing, porosity, bulk density, Cold Crushing Strength (CCS), slag tests were carried out. Apparent porosity and bulk density were measured by Archimedes Method according to ISO EN 993-1 and 993-2 standards. The Cold Crushing Strength tests of samples were done according to ISO ENV 1402-2 standard. CCS tests were carried out in a 200 ton hydraulic press (Atom Technique™, Turkey).

X-ray diffraction (XRD) was conducted using a PHILIPS PAN analytical™ X'Pert PRO X using the setting of 45 mA and 40 kV over a 2θ range between 0-90°. Scanning Electron Microscopy (SEM) investigations were carried out with a JEOL™ T-330 SEM operated at 20 kV and linked with Noran™ Energy Dispersive Spectrometer (EDS) attachment.

RESULTS AND DISCUSSION

Physical and Mechanical Tests

In order to investigate the effect of MgO addition on the properties of the castables and to specify the optimum amount of additives, the mixtures were prepared and sintered at 1500-1600 °C. Water absorption, porosity, bulk density and cold crushing strength (CCS) results obtained are given in Table IV and V, respectively. It can be seen from Tables IV and V that, as expected, the values of CCS and bulk density increase and porosity decreases as the sintering temperature rises. Increasing the sintering temperatures from 1500 to 1600 °C has influenced these properties positively but physical properties improved with the amount of MgO addition up to 5 wt%; after this level there was a negative effect with an increasing amount of MgO addition.

Table III – Particle size distribution and mass contents (wt%) of seawater magnesia added (M3-7) and free from seawater magnesia (M0) castables

Raw materials	Particle Size (mm)	M0 (wt%)	M3 (wt%)	M4 (wt%)	M5 (wt%)	M6 (wt%)	M7 (wt%)
Tabular alumina	1-6	37.20	37.20	37.20	37.20	37.20	37.20
Tabular alumina	0.04-1	35.60	34.60	34.27	33.93	33.60	33.27
MgO	0.04-0.1	-	1.00	1.33	1.67	2.00	2.33
MgO	- 0.04	-	2.00	2.67	3.33	4.00	4.67
Tabular alumina	- 0.04	12.20	10.20	9.53	8.87	8.20	7.53
Secar-71	- 0.04	2.50	2.50	2.50	2.50	2.50	2.50
Micro silica	- 0.04	0.50	0.50	0.50	0.50	0.50	0.50
Reactive alumina	-0.04	7.00	7.00	7.00	7.00	7.00	7.00
Calcined alumina	-0.04	3.97	3.97	3.97	3.97	3.97	3.97
ADS	-0.04	0.50	0.50	0.50	0.50	0.50	0.50
ADW	-0.04	0.50	0.50	0.50	0.50	0.50	0.50
Dispersant	-	0.03	0.03	0.03	0.03	0.03	0.03

Table IV – Physical properties of free from seawater magnesia and seawater magnesia addition of castables at 1500 °C

Refractory properties	M0	M3	M4	M5	M6	M7
Water absorption (%)	5.34	6.96	6.77	6.74	6.98	7.59
Apparent porosity (%)	16.70	20.23	19.78	18.73	20.41	21.74
Bulk density (g/cm^3)	3.13	2.90	2.92	3.00	2.92	2.86
Cold crushing strength (MPa)	93	158	158	170	150	133

Table V – Physical properties of free from seawater magnesia and seawater magnesia addition of castables at 1600 °C.

Refractory Properties	M0	M3	M4	M5	M6	M7
Water absorption (%)	5.26	6.88	6.56	6.05	6.23	6.43
Apparent porosity (%)	16.52	20.18	19.50	17.43	18.15	19.03
Bulk density (g/cm^3)	3.14	2.94	2.97	3.03	3.00	2.96
Cold crushing strength (MPa)	125	178	196	254	222	210

It can be seen from Table V that an addition of 5 wt% MgO resulted in high density and relatively low porosity in the castables. CCS results of castables revealed that the mixture with added 5 wt% MgO showed higher CCS compared to other mixtures. This result can be explained by the fact that $MgAl_2O_4$-spinel structure has lower rigidity and higher yield strength compared to alumina. This makes the alumina-spinel composites attain a stronger structure compared with alumina [23]. Moreover, this can presumably be explained by the fact that the spinel phases formation highly effective on the CCS of castables (Figure 2). However, the increased *in situ* spinel formation in the samples leads to an expansion in its lattice as well as an increase in the porosity. On the other hand, the formation of brucite in the form of castable refractory by reacting with the magnesia and water vapour at 150-200 °C while water is removed from the castable structure during the drying process. [8,9]. As a result of this reaction, 5% of volume expansion occurs in the castable refractory [9,10]. This causes porosity increase in the reactions and it hinders the material from obtaining a more dense structure during the sintering. Consequently, the addition of 5 wt% MgO was determined as the optimum amount.

Phase Analysis

The X-ray diffraction analysis of the refractories uncorroded zone (cold zone) having same particle size distributions indicated the presence of $MgAl_2O_4$-spinel, corundum (α-Al_2O_3) and CA_2 phases. Phase analysis results of the castables are given in Figure 2. Since all added MgO turns into MA-spinel as a result of *in situ* reaction with α-Al_2O_3 at sintering temperature, free MgO is not seen in system.

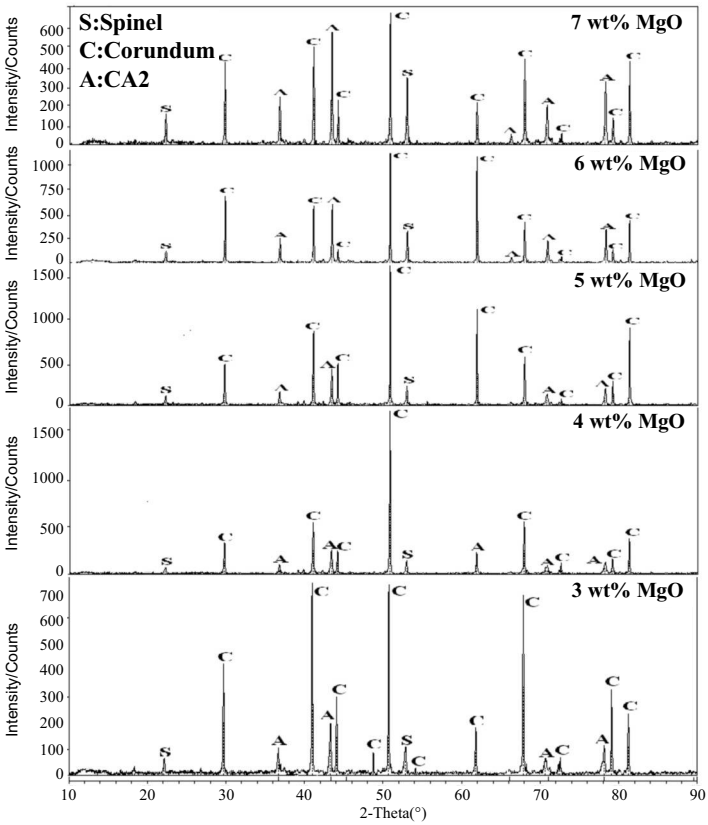


Fig. 2. XRD pattern of MgO added castables sintered at 1600 °C.

Table VI – Chemical composition of ladle slag (%) (C/S = 2.29)

	FeO/Fe_2O_3	SiO_2	MnO	Al_2O_3	CaO	MgO	P_2O_5	S	Na_2O	K_2O	TiO_2	Cr_2O_3
wt%	17.66	14.32	4.62	14.02	32.87	7.01	0.617	0.221	0.001	0.107	0.483	0.114

Although it is observed that there is not a big difference among them, it is realized that this intensity is much higher than the others relative to the refractories added with 5-6-7 wt% MgO.

Slag Corrosion Tests (Crucible Method)

Ladle slag supplied by the steel plant of Erdemir Incorporated, Turkey was used in the corrosion testing of the castable samples. The chemical composition of the slag is given in Table VI. This slag composed mainly of CaO-Al_2O_3-SiO_2, contained a 17.66 wt% iron solution. It was granulated and sifted using a 100 µm sieve. The powdered and sieved slag was separated for use in the corrosion test.

Slag charges were applied to the inside of the castable crucible pot samples prepared according to DIN 51069-2 [24]; one group of samples at 1500 °C and another at 1600 °C were sintered for 4 hours in a furnace with a SFL, UK time controlled direct heater at a heating speed of 10 °C/min. After reaction with the slag, castable samples were sectioned as stated in DIN 51069-2 and their corrosion surfaces were examined. An intense slag region comprising dissolution- and infiltration areas was observed at the interfaces (Figure 3).

For comparison of the slag infiltration in samples M0 and M5, slag infiltration areas were measured using semi-quantitative graph measurement paper. As shown in Figure 4, slag infiltration with no MgO additive castables was higher than the 5 wt% MgO additive at 1600 °C, as expected. However, it can be noted that the slag infiltration of castable M5, although it had higher porosity, was less than that of castable M0.

To examine the slag corrosion in detail, castables M0 and M5 corroded at 1600 °C were investigated. Figure 5a shows the SEM image of the slag region. Figures 6a to 6c show the EDS point analysis extending from the slag contact zone of the same region to the inner sections of the refractory and give the corresponding chemical composition of sample M0. EDS results in the figure are taken from the corroded zone (hot zone), uncorroded refractory zone (cold zone) and the border between the hot and cold zone (border zone). Figures 5b and 7a to 7c indicate respectively, sectional image and details of castable crucible M5 which contained additional MgO.

As seen in the SEM photographs, while the hot zone depth is measured as <4 mm in M0 at the same condition, the hot zone depth of M6 in the corrosion tests also does not exceed 1-2 mm. The effect of the slag to the materials can be explained as the components with low melting points increase the activity of the slag so that it eases the penetration into the materials.

When the SEM-EDS findings are examined (Figures 5a, 5b and Figures 6a, 6b, 6c, Figures 7a to 7c) the complex compound of $(Fe,Mn)(Fe,Al)_2O_4$ is identified as a result of the chemical reactions between Fe^{3+}, Fe^{2+}, Mn^{2+} ions from molten slag existing in the hot zone of the ULC castables. In the hot zone, the existence of Ca^{2+} and Si^{4+} ions is observed as well. The calcium-alumina-silicate vitreous structure which is formed increases the penetration depth.

CONCLUSIONS

1. An increase in the *in situ* spinel formation in samples was determined by XRD containing from 3 to 7% of the castable refractories where $MgAl_2O_4$ spinel formulation was provided.
2. As a result of the physical and mechanical tests, it has been concluded that the content of the MgO changed from 3 wt%, to 5 wt%. In the composition of the

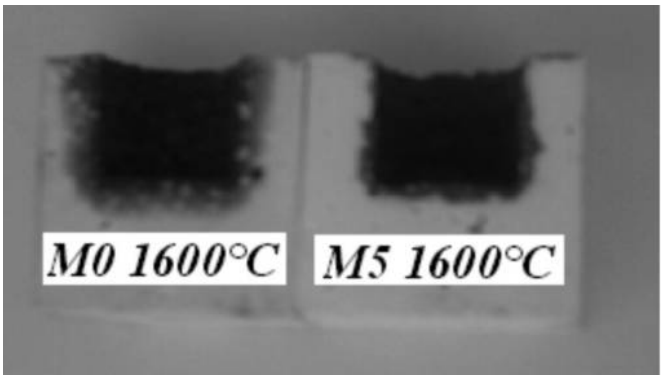


Fig. 3. Slag penetration areas images of M0 (with no MgO additive), M5 (containing 5wt% MgO additive) castables at 1600 °C.

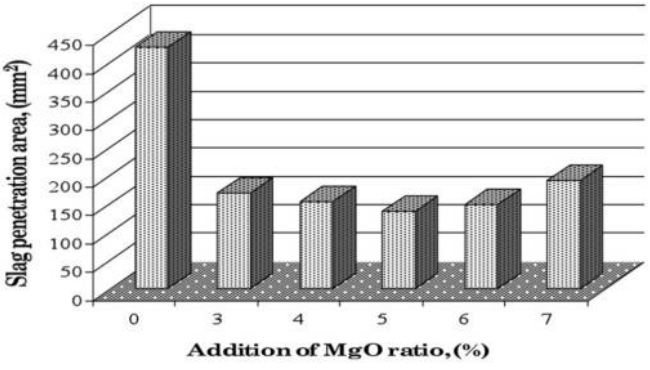


Fig. 4. Slag penetration areas of seawater magnesia added (M3-7) and free from seawater magnesia (M0) castable at 1600 °C.

mixtures, the values of bulk density were observed to increase and porosity to decrease. But the content of MgO was changed from 6 wt%, to 7 wt%. In the composition of the mixtures, the values of CCS and bulk density were observed to decrease and porosity to increase. When the test results of the Cold Crushing Strength were examined, it was determined that *in situ* spinel phase had a positive effect up to 5 wt % MgO but in the 6 and 7 wt% MgO content cold crushing strength decreased as a result of the negative effects of both the brucite formed due to the surrounding moisture and the porosity rise. Consequently, the addition of 5 wt% MgO was determined as the optimum addition amount.

3. The experimental results indicated that the slag penetration decreased with 5 wt% MgO addition.

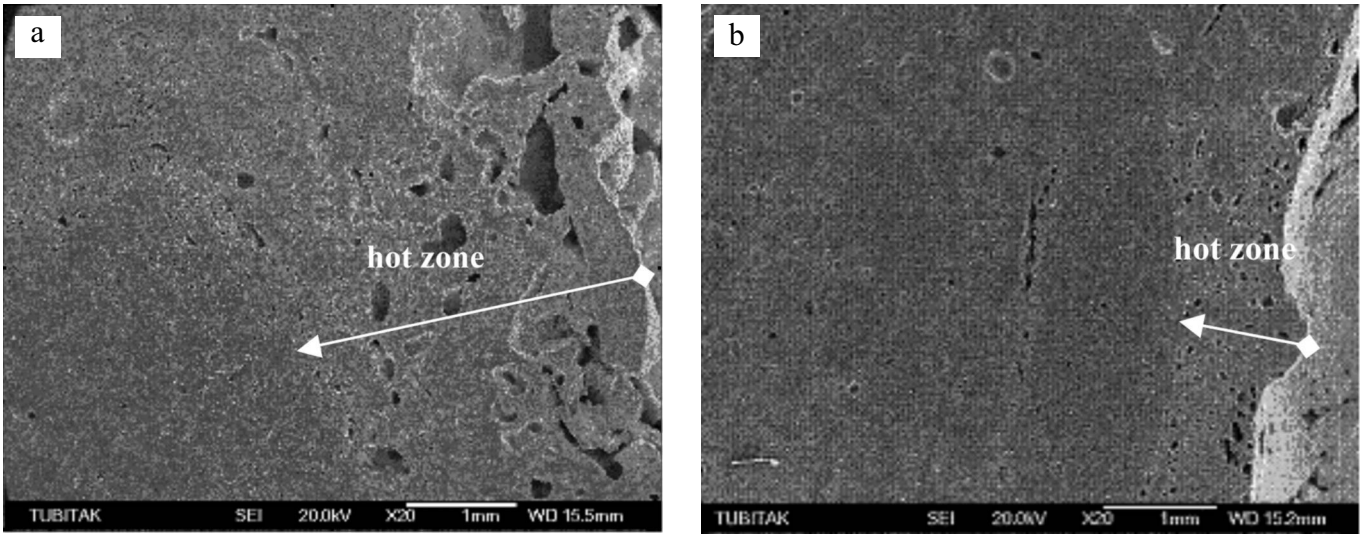
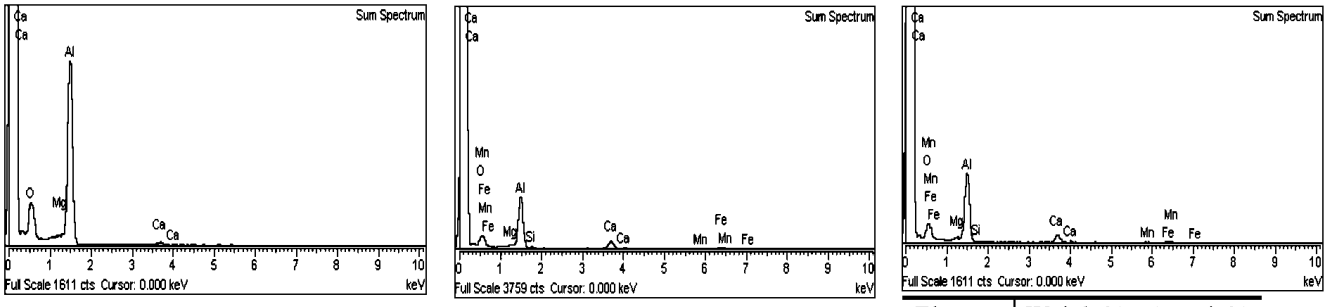


Fig. 5. a-b. SEM micrograph of the sample which were prepared with no MgO additive (M0) and containing 5wt% MgO additive (M5) at hot zone (20×).



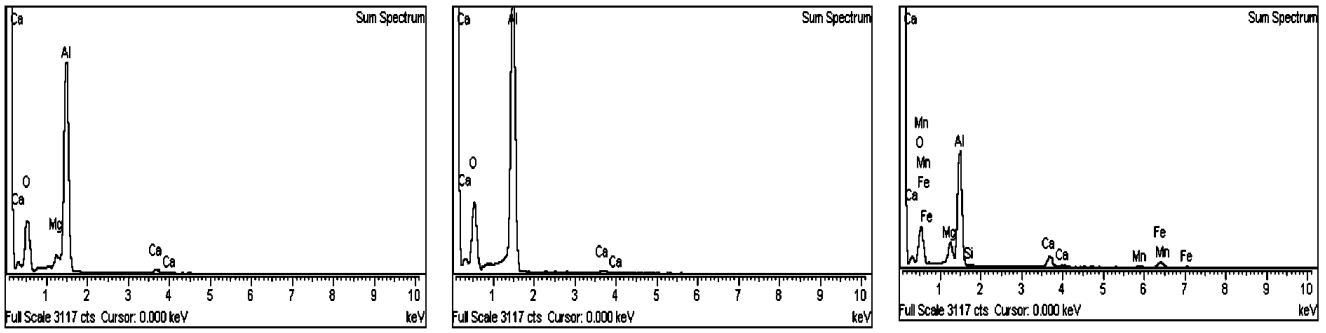
Element	Weight%	Atomic%
O K	36.14	49.02
Mg K	0.23	0.20
Al K	62.15	49.98
Ca K	1.48	0.80

Element	Weight%	Atomic%
O K	37.45	52.96
Mg K	0.83	0.77
Al K	44.09	36.97
Si K	1.28	1.03
Ca K	10.22	5.77
Mn K	1.00	0.41
Fe K	5.13	2.08

Element	Weight%	Atomic%
O K	40.97	56.38
Mg K	1.13	1.02
Al K	43.70	35.66
Si K	0.16	0.13
Ca K	8.21	4.51
Mn K	0.93	0.37
Fe K	4.89	1.93

a) cold zone b) border zone c) hot zone

Fig. 6. a-b-c) EDS analysis of slag penetration layer in M0 castable.



Element	Weight%	Atomic%
O K	40.04	53.09
Mg K	2.80	2.44
Al K	55.32	43.49
Ca K	1.85	0.98
Totals	100.00	

a) cold zone

Element	Weight%	Atomic%
O K	39.54	52.55
Al K	59.73	47.07
Ca K	0.72	0.38
Totals	100.00	

b) border zone

Element	Weight%	Atomic%
O K	35.20	50.29
Mg K	7.39	6.95
Al K	41.07	34.79
Si K	0.78	0.64
Ca K	5.93	3.38
Mn K	1.94	0.81
Fe K	7.68	3.14
Totals	100.00	

c) hot zone

Fig. 7. a-b-c) EDS analysis of slag penetration layer in M5 castable.

4. Castables including $MgAl_2O_4$ spinels have a high melting temperature and exhibited highly effective resistance against the basic slag.

ACKNOWLEDGEMENT

We would like to thank Superateş Refractories Company for their support throughout this investigation.

REFERENCES

1. J. Mori, W. Watanabe, M. Yoshimura, Y. Oguchi, T. Kawakami, “Material Design of Monolithic Refractory for Steel Ladle”, *Amer. Ceram. Soc. Bull*., 1990, vol. 69(7), pp. 1172-1176.
2. W.E. Lee, R.E. Moore, “Evolution of in situ Refractories in the 20th Century”, *J. Amer. Ceram. Soc*., 1998, vol. 81(6), pp. 1385-1410.
3. P. Korgul, D.R. Wilson, W.E. Lee, “Microstructural Analysis of Corroded Alumina-spinel Castables Refractories”, *J. Eur. Ceram. Soc*., 1997, vol. 17, pp. 77-84.
4. C.F. Chan, Y.C. Ko, “A Study of Commercial Magnesia Alumina Spinels for Alumina-Spinel Castables”, *Interceram*, 1998, vol. 47(6), pp. 374-378.
5. C.A. Schacht, *Refractories Handbook*, 2004, Marcel Dekker Inc., New York, pp. 215-257.
6. H. Sarpoolaky, K.G. Ahari, W.E. Lee, “Influence of in situ Phase Formation on Microstructural Evolution and Properties of Castable Refractories”, *Ceram. Int*., 2002, vol. 28, pp. 487-493.
7. S. Mukhopadhyay, P.K. Das Poddar, “Effect of Preformed and in situ Spinels on Microstructure and Properties of a Low Cement Refractory Castable”, *Ceram. Int*., 2004, vol. 30, pp. 369-380.
8. C. Parr, T.A. Bier, M. Vialla, C. Revais, “Revais, an Approach to Formulate Spinel Forming Castables”, *Unitecer99*, 1999, 6-9 September, Berlin-Germany, pp. 19-21.
9. X. Cheng, “Optimization of Magnesia Based Cement Free Spinel Bonded Castables”, PhD Thesis, 1999, Université de Montréal, Canada, December.
10. R. Sarkar, A. Ghosh, S. Das, “Reaction Sintered Magnesia Rich Magnesium Aluminate Spinel: Effect of Alumina Reactivity”, *Ceramic International*, 2003, vol. 29, pp. 407-411.
11. T. Yamamura, Y. Hamazaki, T. Kaneshige, T. Toyoda, M. Nishi and H. Kato, “Alumina-Spinel Castable Refractories for Steel Teeming Ladle”, *Taikabutsu Overseas*, 1992, vol. 12(1), pp. 21-27.
12. M.W. Vance, G.W. Kriechbaum, R.A. Henrichsen, G. Maczura, K.J. Moody, S. Munding, “Influence of Spinel Additives on High Alumina/Spinel Castables”, *Bull. Amer. Ceram. Soc*., 1994, vol. 73(11), pp. 70-74.
13. Y.C. Ko, “Role of Spinel Composition in the Slag Resistance of Al_2O_3–Spinel and Al_2O_3–MgO Castable”, *Ceram Int.*, 2002, vol. 28, pp. 805-810.
14. P. Korgul, D.R. Wilson, W.E. Lee, “Microstructural Analysis of Corroded Alumina-Spinel Castable Refractories”, *J. Europ. Ceram Soc*., 1997 vol. 17, pp. 77-84.
15. J. Mori, W. Watanabe, M. Yoshimura, Y. Oguchi, T. Kawakami, “Material Design of Monolithic Refractories for Steel Ladle”, *Bull. Amer. Ceram. Soc*, 1990, vol. 69(7), pp. 1172-1176.
16. L.A. Diaz, R. Torrecillas, A.H. de Aza, P. Pena, “Effect of Spinel Content on Slag Attack Resistance of High Alumina Refractory Castable”, *J. European Ceram. Soc*., 2007, vol. 27, pp. 4623-4631.

17. L.A. Diaz, R. Torrecillas, A.H. de Aza, P. Pena, S. de Aza, "Alumina –rich Refractory Concretes with Added Spinel, Periclase and Dolomite: A Comparative Study of Their Microstructural Evolution with Temperature", *J. European Ceram. Soc*., 2005, vol. 25, pp. 1499-1506.
18. S. Banerjee, *Monolitic Refractories, A Comprehensive Handbook*, 1998, World Scientific Publishing.
19. H. Sarpoolaky, K.G. Ahari, W.E. Lee, "Influence of in situ Phase Formation on Microstructural Evaluation and Properties of Castable Refractories", *Ceramics International*, 2002, vol. 28, pp. 478-493.
20. W.E. Lee, W. Vieira, S. Zhang, K.G Ahari, H. Sarpoolaky, C. Parr, "Castable Refractory Concretes", *Int. Mater. Rev*., 2001, vol 46(3), pp. 145-167(23).
21. A. Nishikawa, *Technology of Monolitic Refractories*, Plibrico Japan Company Limited, (1984).
22. F. Simonin, C. Olagnon, S. Maximilien, G. Fantozzi, "Thermomechanical Behaviour of High-alumina Refractory Castables with Synthetic Spinel Addition", *J. Am. Ceram. Soc.*, 2000, vol. 83(10), pp. 2481-2490.
23. D.R. Dinger and J.E. Funk, "Particle Packing II-Review of Packing of Polydisperse Particle Systems", *Interceram*, 1992, No. 2, p. 41.
24. D.R. Dinger and J.E. Funk, "Particle Packing III-Discrete Versus Continuous Particle Size, *Interceram*, 1992, No. 5, p. 41.
25. Y.K. Kalpakli, "Effects of Partıcle Size Distrıbutıon on the Refractory Properties and Corrosion Mechanism of Ultra-Low Cement Castables (ULC)", *Proceedings of 12th International Materials Symposium (IMSP'2008)*, October 15-17, 2008, Denizli, Turkey.
26. G. Brandt, M. Mikus, "An Electron Microprobe and Cathod Luminescence Study of Chemical Reactions between Tool and Work Piece When Turning Steel with Alumina-based Ceramics", *Wear*, 1987, vol. 115, pp. 243-263.
27. DIN 51069 Blatt 2: Prüfung keramischer Roh- und Werkstoffe; Vergleichende Prüfung des Verhaltensfeuerfester Werkstoffe gegen den Angriff fester und flüssiger Stoffe bei hoher Temperatur Tiegelverfahren (TV), Nov. 1972.